Relevant achievements on the activities of *fib* WP 2.4.1 for Modelling of Fibre Reinforced Concrete Structures

Joaquim A. O. Barros [1]

[1] Full Prof., ISISE, ARISE, Department of Civil Engineering, University of Minho, Azurém 4800-058 Guimarães, Portugal, barros@civil.uminho.pt

Abstract

The *fib* WP 2.4.1 is a technical committee of the *fib* organization (https://www.fib-international.org/commissions/com2-analysis-design.html) dedicated to the development of methodologies for the design of fibre reinforced concrete (FRC) structures using computer programs based, mainly, on the finite element method (FEM). For taking advantage of the fibre reinforcement, these computer programs should simulate the relevant fibre resisting mechanisms, mainly the ones that increase the post-cracking tensile capacity of cement-based materials. Several challenges are, however, faced for assuring reliable simulations, namely: 1) the knowledge of the stress-crack opening simulating correctly the post-cracking tensile behaviour of the FRC of the structure to be designed; 2) modelling the contribution of fibre reinforcement in structures failing in shear, punching or torsion; 3) level of accuracy of these models on performing the serviceability and ultimate limit state design verifications; 4) guarantee results independent of the refinement of the finite element mesh; 5) design format (characteristic, average or design values for the material properties). To contribute for a proper handling of some of these challenges, the *fib* WP 2.4.1 has been coordinating a series of blind simulation competitions, whose relevant objectives and results are described in this paper. The vison on the use of this information for deriving information useful in the design of FRC structures is also provided.

Keywords: Fibre reinforced concrete; finite element method; nonlinear finite element analysis; Blind simulation competition.

1- INTRODUCTION

Research and real applications have shown the potential of the addition of discontinuous (short) fibres to cement based materials on the significant improvement of the behaviour of concrete structures at serviceability and ultimate limit state conditions (SLS and ULS, respectively) [1, 2]. The structures made by fibre reinforced concrete (FRC) and including conventional reinforcements will be herein referred by the acronymic R/FRC structures. Regarding SLS, it should be highlighted the smaller concrete crack width and stress level in conventional reinforcements and the higher stiffness of FRC structures during their elasto-cracked stage [1, 3-8]. For ULS, it should be indicated the higher load carrying capacity, more ductile failure modes and larger energy absorption and dissipation capacity and structural integrity under loading conditions representative of extreme events [1, 9-22]. The fibre reinforcement also provides significant enhancements in the durability [22-30] and life cycle of concrete structures [31-34]. The main applications of FRC are still concentrated in flooring, tunnelling and in some pre-fabrication [1, 35-43], being too scarce in the development of innovative structural systems where the benefits of the fibre reinforcement mechanisms have recognized potential for obtaining technical and economic advantages regarding conventional systems.

The fibres, when crossed by cracks, develop reinforcement mechanisms through to their pull-out resistance, whose effectiveness depends on their material and geometric properties, on the mechanical properties of the surrounding cement paste, and on the fibre distribution and orientation in the element. These last ones are dependent on the technology of FRC application, its rheological properties and geometry of the element to produce [44].

Due to these complex phenomena, modelling the fibre reinforcement benefits should be based in computational models that simulate the behaviour of FRC from the fresh up to its hardened stages [45-54]. Commercial software based on the finite element method (FEM) have been used for the simulation of the material nonlinear behaviour of FRC structures, as the contribution of fibre reinforcement is, mainly, activated after the fibres have been crossed by cracks. Smeared and discrete crack approaches (SCM, DCM), strong embedded discontinuity methods (ESD), and elasto-plastic-damage models are the most current models in these software [45-54]. However, the applicability of these approaches has been assessed by simulating experimental tests with elements, in general, of small scale, where the values of their model's parameters are adjusted for the aimed predicting level, constituting, therefore, an inverse technique of very small utility for structural design practice. The major part of these models considers the contribution of fibre reinforcement mechanisms through a cohesive traction-separation law obtained from semi-empirical recommendations, or from experimental results, directly or from inverse analysis [55]. However, there is still considerable uncertainty regarding the most adequate methodology to derive the model's parameters values for predicting accurately the behaviour of a given structure. An inadequate assessment of these values provides results without any representativeness of the real behaviour of the structure. Furthermore, available information in this respect shows that the σ-w relationships derived from IA provides unsafe predictions [56].

The relative reduced use of computational tools for exploring the advantages of FRC on the development of competitive and sustainable R/FRC solutions are due to the following main reasons: 1) lack of preparation on the use of the available models; 2) lack of understanding of the impact of the relevant parameters of the models on the prediction of the behaviour of a R/FRC structure; 3) difficulties on transforming experimental results obtained in recommended quality control tests in reliable data for the constitutive models.

The *fib* WP 2.4.1 - Modelling of Fibre Reinforced Concrete Structures was established with the main aim of developing guidelines on the use of FEM-based software for the design of R/FRC structures. The execution of blind simulation competitions (BSC) is part of this strategy, by obtaining information about the reliability of constitutive models available in commercial and in-house software, as well as their proper use, in the analysis and design of R/FRC structures.

This work describes the BSC already carried out, and discuss other activities planned to be executed with the obtained information for assessing the influence of the relevant model parameters towards a more comprehensive use of them under the framework of reliable and safe design methodologies.

2- BLIND SIMULATION COMPETITIONS

2.1 - Introduction

Under the framework of the *fib* WP 2.4.1, the BSC have the following main objectives: 1) obtain reliable experimental data for the assessment of the potentialities and debilities of FEM-based constitutive models on the analysis and design of FRC structures; 2) by considering this data, perform parametric studies and sensitivity analysis for assessing the influence of the models parameters on their predictive performance; 3) collect this experimental data in a Web-based information platform (WeBIP) for the use of Machine Learning (ML) algorithms to provide the most appropriate values for the most used classes of FEM-based models on the design of FRC structures.

The type of structures for the BSC was selected considering the already recognized level of fibre reinforcement efficiency, namely: 1st BSC – fibre reinforcement for the total replacement of steel stirrups in beams failing in shear [1, 2, 35, 57-66]; 2nd BSC – fibre reinforcement for partial replacement of conventional flexural reinforcement in slabs supported on piles or columns [1, 2]; 3rd BSC – fibre reinforcement for the total replacement of conventional transverse reinforcement in RC slabs failing in punching [67-70]. The last BSC, to be executed in 2024, will be dedicated to exploring the use of high-performance fibre reinforced concrete (HPFRC) and hybrid reinforcement (fibre reinforced polymers, FRP, and steel bars) applied with or without a certain prestress level for the development of elements of thin wall tubular cross section. By disposing this hybrid reinforcement properly, it is aimed to eliminate all transverse reinforcement for the shear and torsional effects, since they are those most susceptible to corrosion, which allow to significantly decrease the wall thickness of this type of elements, resulting lightweight elements.

For the appraisal of the predictive performance of existing FEM-based constitutive models, an intensive structural monitoring system is used, like Digital Image Correlation (DIC) for assessing crack width, crack spacing and strain field, electric strain gauges for measuring the strains in critical regions, mainly on conventional reinforcements, and displacements transducers for registering the deformation of the structure.

2.2 - 1st BSC: steel-fibre reinforced concrete beams failing in shear

Figure Figure 1 shows a sketch of the geometry of the specimen, support and loading conditions.

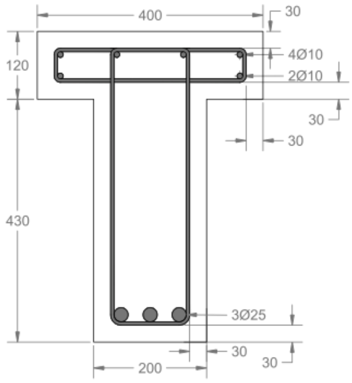

(a)

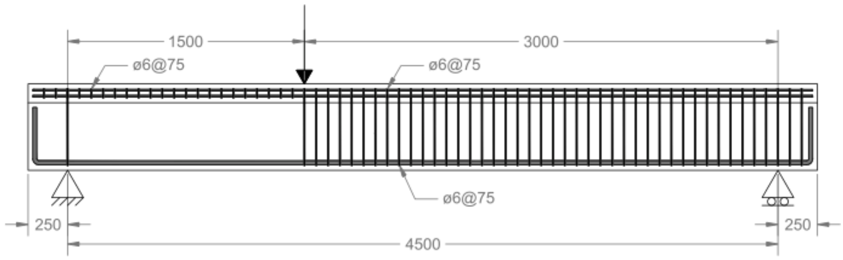

(b)

Figure 1 - Geometry of the beam: (a) cross-section, and (b) longitudinal view (dimensions in mm).

The composition of the steel fibre reinforced concrete (SFRC) corresponds to a concrete C50/60 XD3 (P) CL 0.20 D_{max} 12.5 S5, with a type cement CEM II/A-L 42.5R of fast hardening of 58.8 and 67.1 MPa at seven and 28 days, respectively. Hooked end steel fibres of 33 mm length, 0.55 mm diameter and tensile strength higher than 1100 MPa were used. At 14 days, this SFRC has presented an average compressive strength in 4 standard cylinders of 64.2 MPa [1.5 MPa] (NP EN 12390-3:2011 [71]), a modulus of elasticity of 32.9 GPa [0.4 GPa] (NP EN 12390-13:2014 [72]). By performing three-point bending tests (3PNBBT) in 6 notched SFRC beams according to the *fib* Model Code 2010 [73], it was obtained an average value for the residual flexural strength parameter at crack mouth opening displacement, CMOD, of 0.5 and 2.5 mm of, respectively, $f_{R,1m}$ =4.79 MPa [0.70 MPa] and $f_{R,3m}$ =3.16 MPa [0.52 MPa]. The values into [] are the standard deviation. The load versus CMOD curves are displayed in Figure 2.

The yield stress and tensile strength of the steel bars [74] of 6, 10 and 25 mm diameter adopted for the stirrups (6 mm) and longitudinal reinforcements (10 mm in the top and 25 mm in the bottom) were 527 MPa [11 MPa] and 700 MPa [16 MPa] (6 mm) 538 MPa [7 MPa] and 696 MPa [6 MPa] (10 mm) and 557 MPa [2 MPa] and 678 MPa [1 MPa] (25 mm).

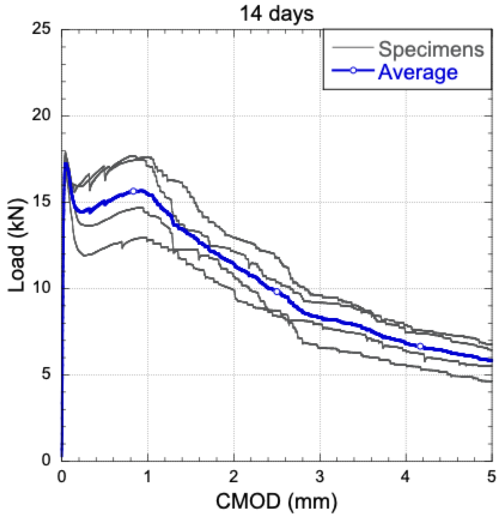

Figure 2 - Load versus crack mouth opening displacement (CMOD) relationships in the three-point notched beam-bending tests executed at 14 days.

Two twin beams were subjected to eccentric loading under displacement control of 50µm/s at the loaded section, until failure. Deflection (displacement of the cross-section at which the load is applied), load and concrete strain at the level of the longitudinal reinforcement in the loaded section were measured during the tests (Figure

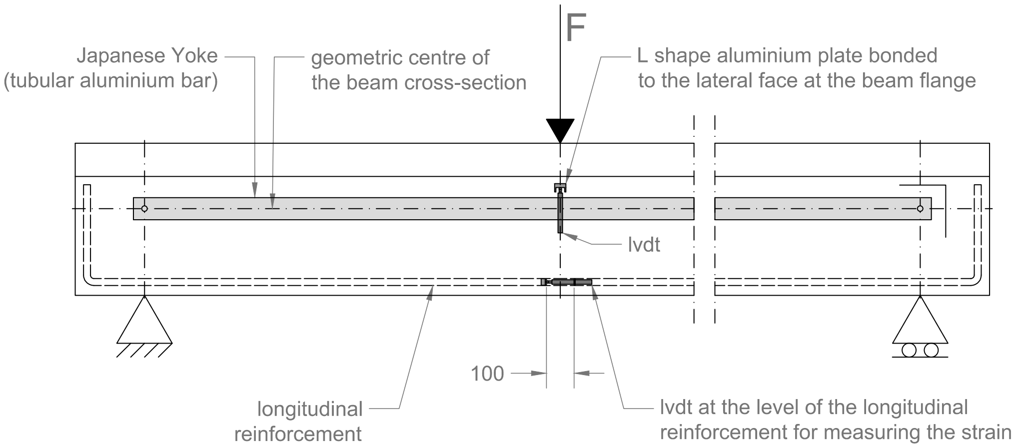

Figure). The strain was determined by dividing the displacement recorded in the displacement transducer (LVDT) by its stroke (100 mm).

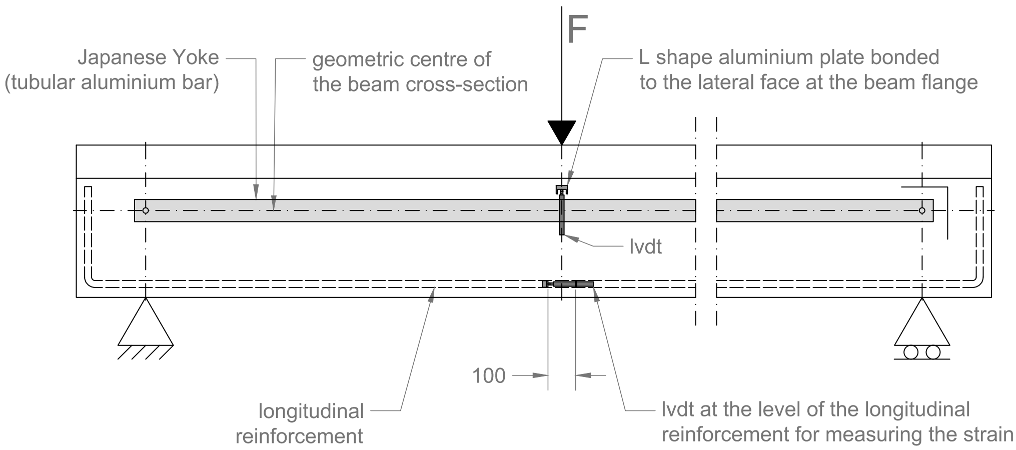

Figure 3 – Schematic representation of the monitoring system to register the beam's deflection in the loaded section and the concrete strain at the level of the bottom longitudinal reinforcement. (dimensions in mm).

Figure 4 displays the experimental results. Unfortunately, the record of the strain of the first beam was lost. Figure 5 represents the crack pattern at failure of both tested beams, which shows that each beam failed in shear.

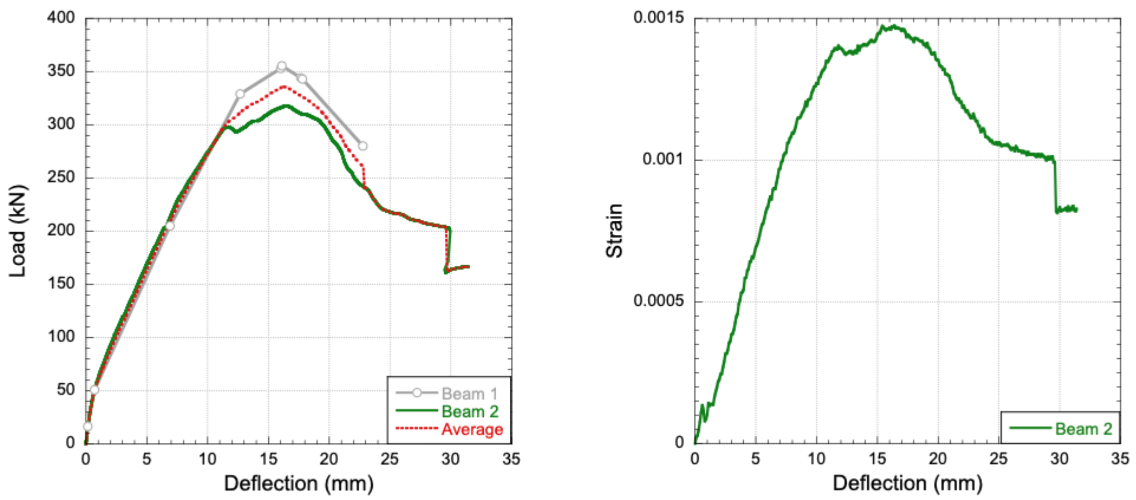

(a) (b)

Figure 4 - Experimental results in terms of deflection at the beam's loaded section versus: (a) load; (b) and concrete strain at the level of the longitudinal reinforcement.

(a) (b)

Figure 5 - Crack pattern at failure in the short shear span region of beam: (a) 1; and (b) 2

Five different classes of models were used by the participants, namely: Smeared Crack Models (SCM), 46%; Discrete Crack Models (DCM), 8%; Concrete Damage Plasticity (CDP), 30%; Lattice Discrete Particle Models (LDPM), 5%; Others, 11%.

Figure 6 shows the experimental average, the individual numerical predictions, and their envelope for the load versus deflection and strain versus deflection up to the deflection corresponding to the end of the experiments.

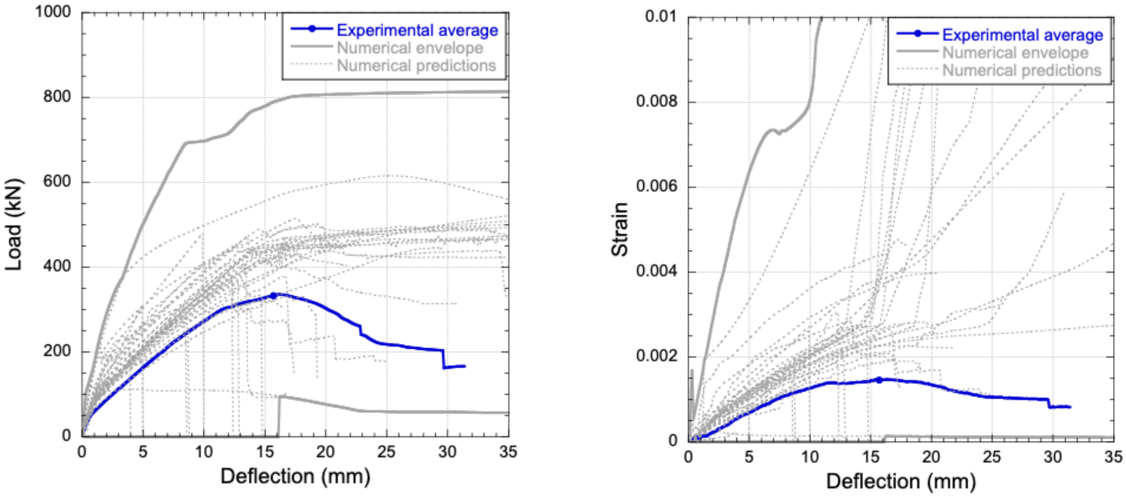

(a) (b)

Figure 6 - Experimental results, numerical envelope, and numerical predictions of all participants in terms of: (a) load versus deflection, and (b) strain versus deflection.

Although the two first ranked participant teams have used SCM, the dispersion on the predictions with this class of models was very high. The predictive performance of the proposals where commercial software was used was better and with smaller dispersion than in the proposals where in-house software was utilized. Despite the provided experimental data for the definition of the relevant models' parameters, inaccuracies on the load capacity, deflection and strain at peak load have attained 40%, 113% and 600%, respectively. Furthermore, inadequate failure modes have been estimated, and simulations with the same commercial software have provided very different results. A more detailed analysis of the results can be found elsewhere [75].

2.3 – 2nd BSC: continuous shallow R/SFRC beams failing in bending

The main objective of this BSC is to simulate the behaviour of a region in the alignment of columns/piles of an R/SFRC slab. In this application, the conventional flexural reinforcement ratio is relatively small, therefore flexure is, in general, the governing failure mode. In slabs supported on piles of industrial buildings where forklifts can elevate objects relatively high for their stockage, an incorrect evaluation of the deflection at SLS conditions can lead to accidents during those operations. Crack width must also be estimated with sufficient precision to avoid durability concerns and to mobilize efficiently the aggregate interlock resisting mechanism to assure the intended shear and punching capacities provided exclusively by the FRC. Therefore, in this 2nd BSC, special focus was given on the predictions of data concerning SLS verifications.

Figure 7 shows a sketch of the geometry of the specimen, including the details of the support and loading conditions. The specimen consists of a continuous shallow beam of two equal spans and same rectangular cross-section, reinforced with longitudinal bars at the bottom and top over the central support (the latter limited to the hogging region). In the region of the highest positive bending moment (sagging region), a higher percentage of reinforcement is provided in each span.

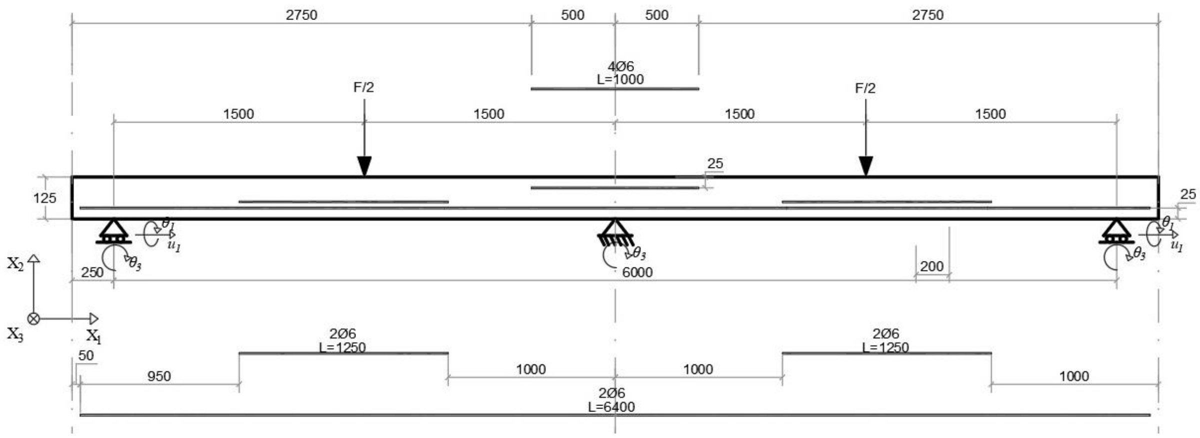

(a)

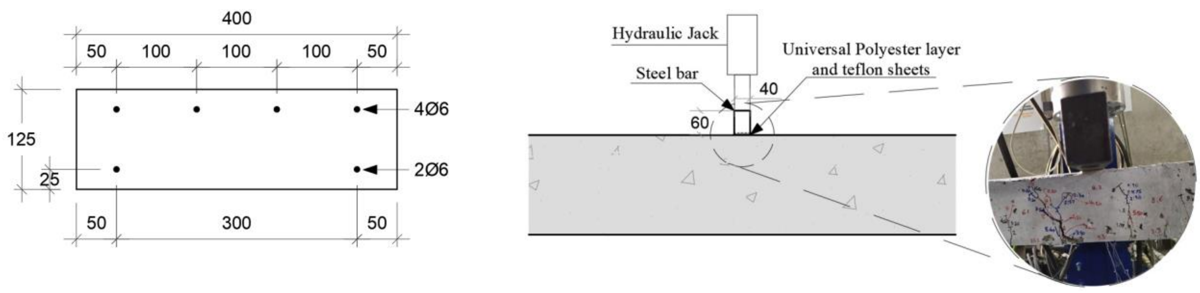

(b) (c)

Figure 7 - Geometry of the specimen: (a) longitudinal view; (b) cross-section in the hogging region; and (c) detail of the loading conditions (dimensions in mm).

Regarding the mix composition of the 2nd BSC, it was the same adopted in the 1st BSC, apart the type of cement, which was now a CEM I 52.5R of fast hardening of 30 and 52.5 MPa at 2 and 28 days, respectively, and the hooked end steel fibres that had a length of 60 mm, a diameter of 0.9 mm and tensile strength higher than 1900 MPa. At 19 days, this SFRC presented an average compressive strength in 4 standard cylinders of 57.8 MPa [1.0 MPa] (NP EN 12390-3:2011 [71]), a modulus of elasticity of 31.9 GPa [0.4 GPa] (NP EN 12390-13:2014 [72]). By executing 6 3PNBBT [73] at 19 days, it was obtained $f_{R,1m}$=6.2 MPa [1.5 MPa] and $f_{R,3m}$ =7.6 MPa [1.4 MPa]. The load versus crack mouth opening displacement (F-CMOD) curves are displayed in Figure 8.

The modulus of elasticity, yield stress and tensile strength of the steel bars of 6 mm diameter and ribbed surface used for the flexural reinforcement, determined experimentally [74], was, respectively, 222199 MPa, 627.25 MPa and 769.57 MPa with a STD of 14970 MPa, 15.41 MPa and 13.27 MPa, respectively.

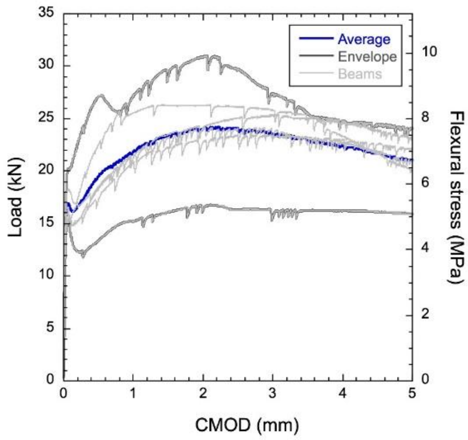

Figure 8 - CMOD versus load and flexural stress in the three-point notched beam-bending tests at 19 days of the SFRC adopted in the 2nd BSC (all tests, envelope, and average curve).

Figures 9 and 10 show the monitoring system for measuring the deflection (by LVDT), the applied load (load cells), strains in SFRC and steel bars (electric strain gauges), and average crack width in the hogging and sagging regions (Digital Image Correlation, DIC).

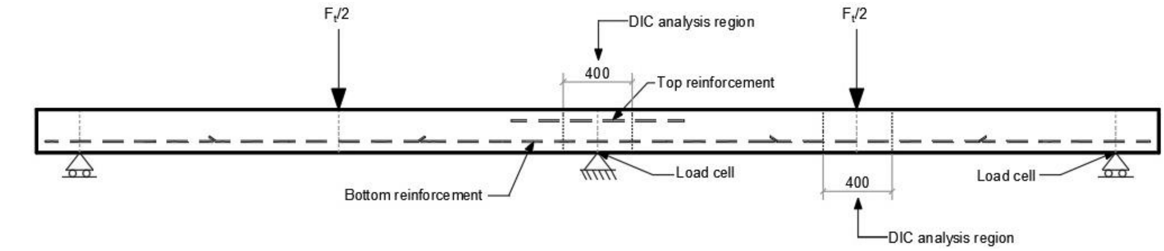

(a)

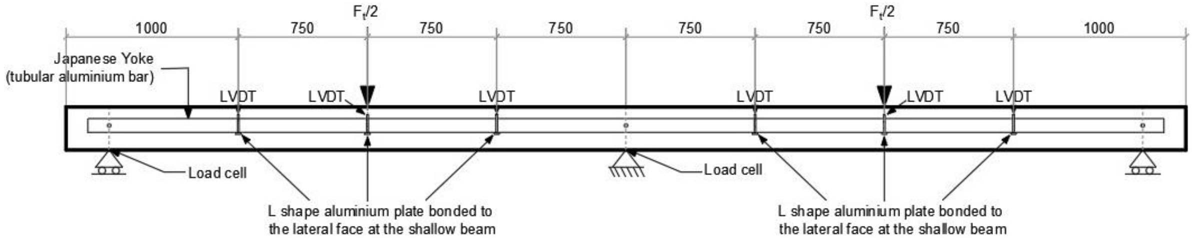

(b)

(c)

Figure 9 - Monitoring systems for measuring the deflection, reaction forces and average crack width in the sagging and hogging regions of the shallow beam: (a) Front view; (b) Rear view; and (c) Photo of the front and rear view of the prototype in the test setup (dimensions in mm).

Figure 11a presents the deflection versus total load ($\bar{u}$ - F_t) obtained experimentally in each shallow R/SFRC beam, as well as this average relationship. Figure 11b shows the relationship between the deflection and the average crack width in the sagging and hogging regions at the level of the tensile reinforcement ($\bar{u}$ - $\bar{w}_S$ / $\bar{w}_H$) of the second shallow beam (the one of the first beam was lost). Figure 11c presents the relationship between the deflection and the strain in the longitudinal tensile reinforcement in the sagging and hogging regions ($\bar{u}$ - $\varepsilon_{s,S}$ / $\varepsilon_{s,H}$). Figure 11d shows the relationship between the deflection and the compressive strain in the SFRC at the loaded section and over the intermediate support, $\bar{u}$ - $\varepsilon_{c,S}$ / $\varepsilon_{c,H}$. As expected, both tested shallow beams failed in bending. A critical analysis of these results can be found elsewhere [76].

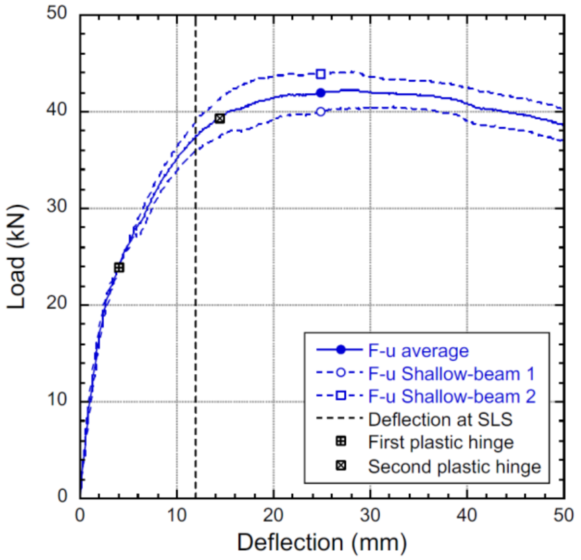

(a)

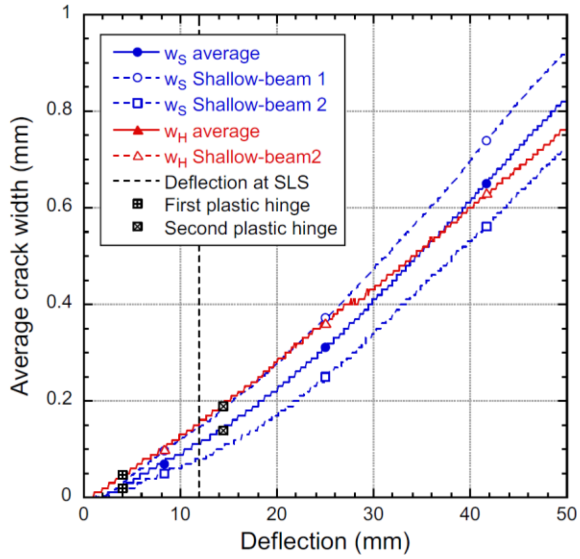

(b)

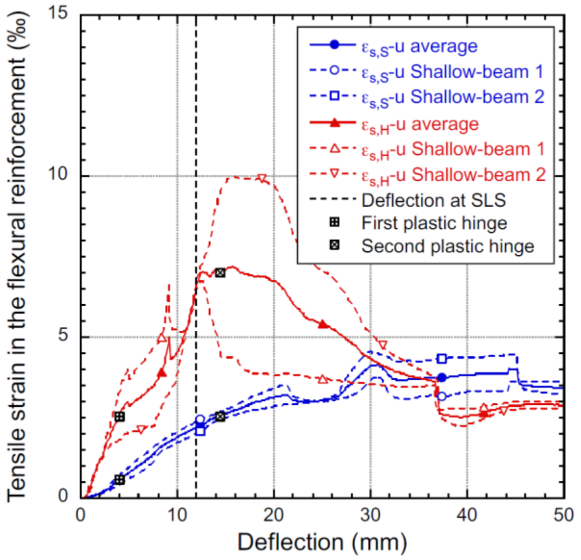

(c)

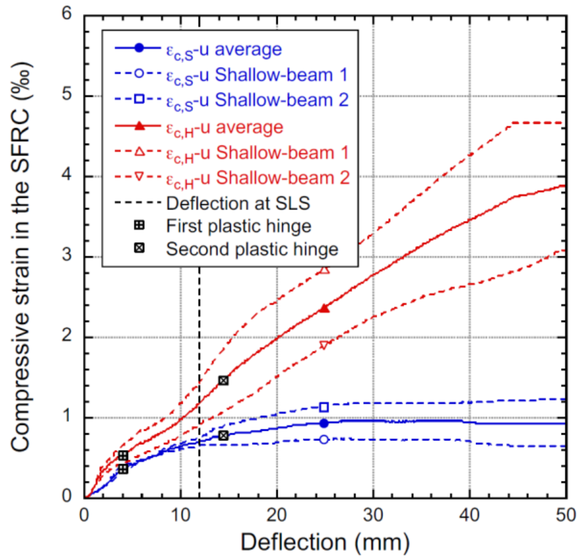

(d)

Figure 11 - Experimental results and average curves of: (a) average deflection versus total load ($\bar{u}$ - F_t), (b) average deflection versus average crack width in the sagging region ($\bar{u}$ - $\bar{w}_S$) and in the hogging region ($\bar{u}$ - $\bar{w}_H$), at the level of the corresponding tensile reinforcement, (c) average deflection versus tensile strain in the flexural reinforcement at the loaded section ($\bar{u}$ - $\varepsilon_{s,S}$) and over the intermediate support ($\bar{u}$ - $\varepsilon_{s,H}$), and (d) average deflection versus compressive strain in the SFRC at the loaded section ($\bar{u}$ - $\varepsilon_{c,S}$) and over the intermediate support ($\bar{u}$ - $\varepsilon_{c,H}$).

Figure 12 includes the curves of load versus deflection, and the average crack width in the hogging and sagging regions versus deflection. Figure 13 presents the curves of tensile strain in the flexural reinforcement at the loaded section and over the intermediate support versus deflection, and compressive strain in the SFRC at the loaded section and over the intermediate support versus deflection. The results are displayed up to the deflection corresponding to the end of the experiments.

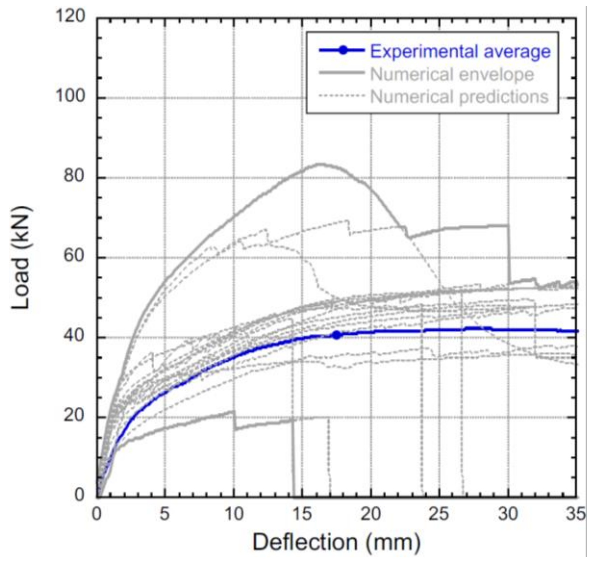

(a)

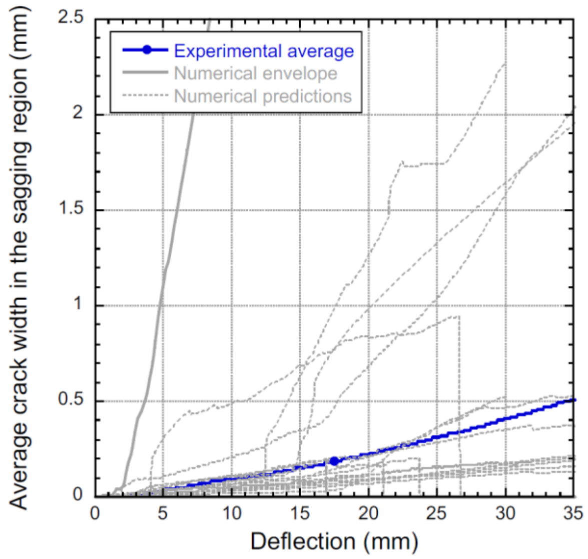

(b)

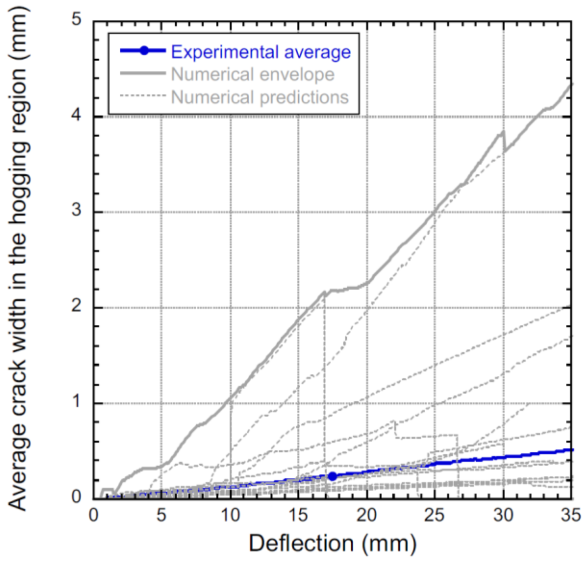

(c)

Figure 12 - Experimental results, numerical envelope and numerical predictions of all participants regarding the: (a) load versus deflection ($\bar{u}$ - F_t), (b) average crack width in the sagging region versus deflection ($\bar{u}$ - $\bar{w}_S$), and (c) average crack width in the hogging region versus deflection ($\bar{u}$ - $\bar{w}_H$).

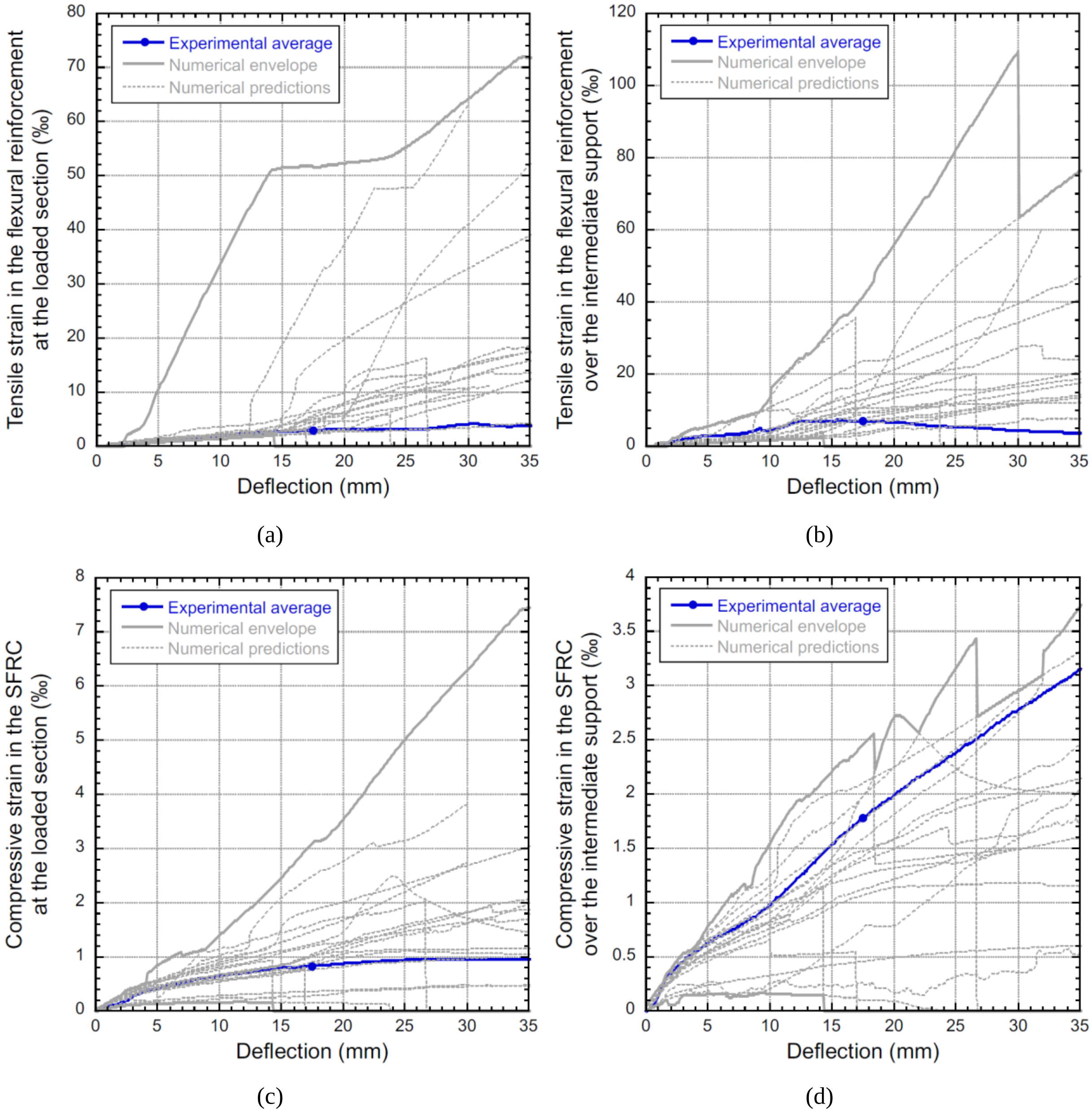

Figure 13 - Experimental results, numerical envelope and numerical predictions of all participants regarding the: a) tensile strain in the flexural reinforcement at the loaded section versus deflection ($\bar{u}$ - $\varepsilon_{s,S}$), b) tensile strain in the flexural reinforcement over the intermediate support versus deflection ($\bar{u}$ - $\varepsilon_{s,H}$), c) compressive strain in the SFRC at the loaded section versus deflection ($\bar{u}$ - $\varepsilon_{c,S}$), and d) compressive strain in the SFRC over the intermediate support versus deflection ($\bar{u}$ - $\varepsilon_{c,H}$).

The normalised mean square root, $NRMS_F$, of the numerical prediction of the load was calculated as:

$$NRMS_F = \frac{1}{F_{\exp}^{\max}} \sqrt{\frac{\sum_{k=1}^{n} \left(F_{\exp}^{k} - F_{num}^{k}\right)^2}{n}} \quad (1)$$

where *k* corresponds to the records, $F_{\exp}^{k}$ and F_{num}^{k} are the experimental and numerical load values of record *k*, respectively, *n* is the number of scan readings, and $F_{\exp}^{\max}$ is the maximum of the experimental load. Equivalent equations are used to compute the *NRMS* of the tensile strain in the flexural reinforcement at the loaded section, $NRMS_{\varepsilon_{s,S}}$, compressive strain in the SFRC at the loaded section, $NRMS_{\varepsilon_{c,S}}$, tensile strain in the flexural reinforcement over the intermediate support, $NRMS_{\varepsilon_{s,H}}$, compressive strain in the SFRC over the intermediate support, $NRMS_{\varepsilon_{c,H}}$, average crack width in the sagging region, $NRMS_{\bar{w}_S}$, and average crack width in the hogging region, $NRMS_{\bar{w}_H}$. The score of each participant was calculated according to the following expression:

$$\text{Score} = 0.2NRMS_F + 0.1NRMS_{\varepsilon_{s,S}} + 0.1NRMS_{\varepsilon_{c,S}} + 0.1NRMS_{\varepsilon_{s,H}} + 0.1NRMS_{\varepsilon_{c,H}} + 0.2NRMS_{\bar{w}_S} + 0.2NRMS_{\bar{w}_H} \quad (2)$$

From the obtained results it can be pointed out the main following observations:

1) The average error (normalised mean square root, *NRMS*) on the numerical predictions in terms of the load, tensile strain in the flexural reinforcement at the loaded section, compressive strain in the SFRC at the loaded section, tensile strain in the flexural reinforcement over the intermediate support, compressive strain in the SFRC over the intermediate support, average crack width in the sagging region, and average crack width in the hogging region was, respectively, 0.29, 2.04, 0.63, 1.96, 0.27, 1.24 and 0.91 (a perfect simulation would correspond to *NRMS* =0);
2) The DCM and the CDP provided the best and worst predictive performances, respectively;
3) In-house software has assured best predictive performance than commercial software;
4) The LDPM and DCM have best predicted almost all the variables of the competition than the SCM and CDP;
5) The larger difference in terms of predictive performance of the LDPM and DCM versus SCM and CDP was mainly on the strains in the steel reinforcements and average crack width.

2.4 – Other planned blind simulation competitions

2.4.1 – 3rd BSC: slabs reinforced with conventional flexural reinforcement and steel fibres, subjected to punching loading configuration

The main objective of this BSC, whose structural tests are planned to be executed in July 2023, is to assess the performance of FEM-based models for predicting the behaviour of flat slabs under punching loading conditions, where fibres are used as a punching/shear reinforcement. This assessment will be, mainly, in terms of force-deflection, deflection profile, and strain levels in conventional flexural reinforcement and in concrete of critical regions of R/SFRC slab. The predictive capacity in terms of crack pattern and failure mode will be also an objective.

The twin prototypes to be tested, whose details are shown in Figure 14, represent a region over a column of an elevated slab or over a pile of a slab supported on piles made by SFRC and including conventional flexural reinforcement in the alignment of columns/piles.

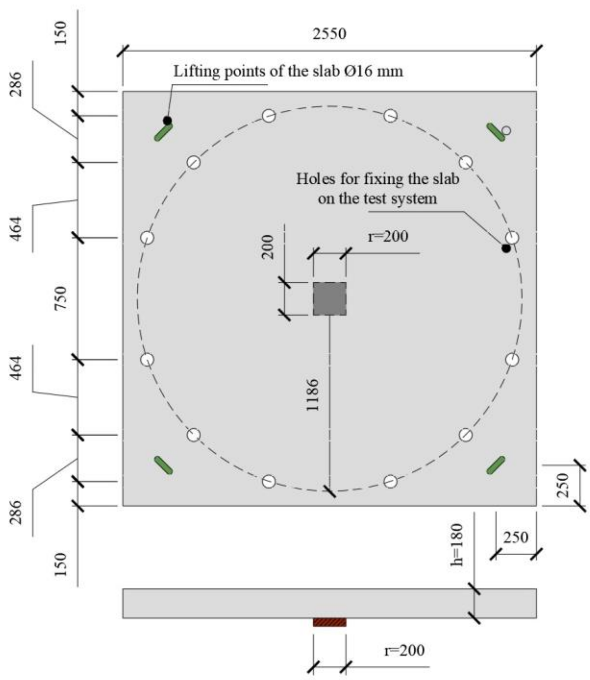

(a)

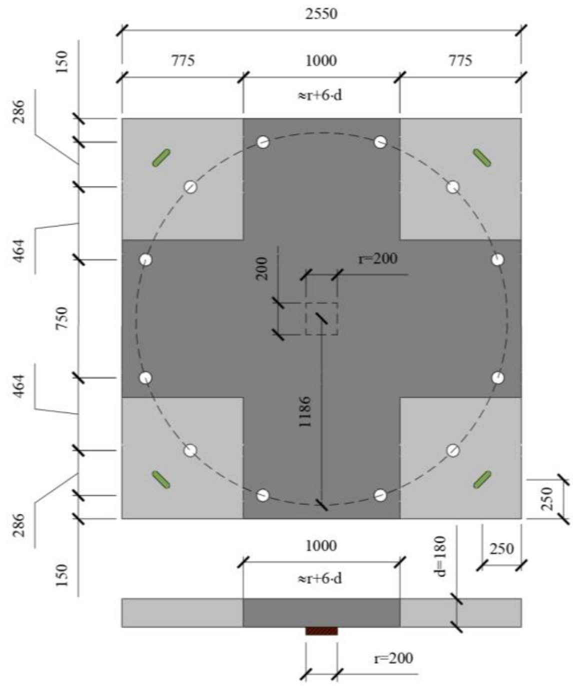

(b)

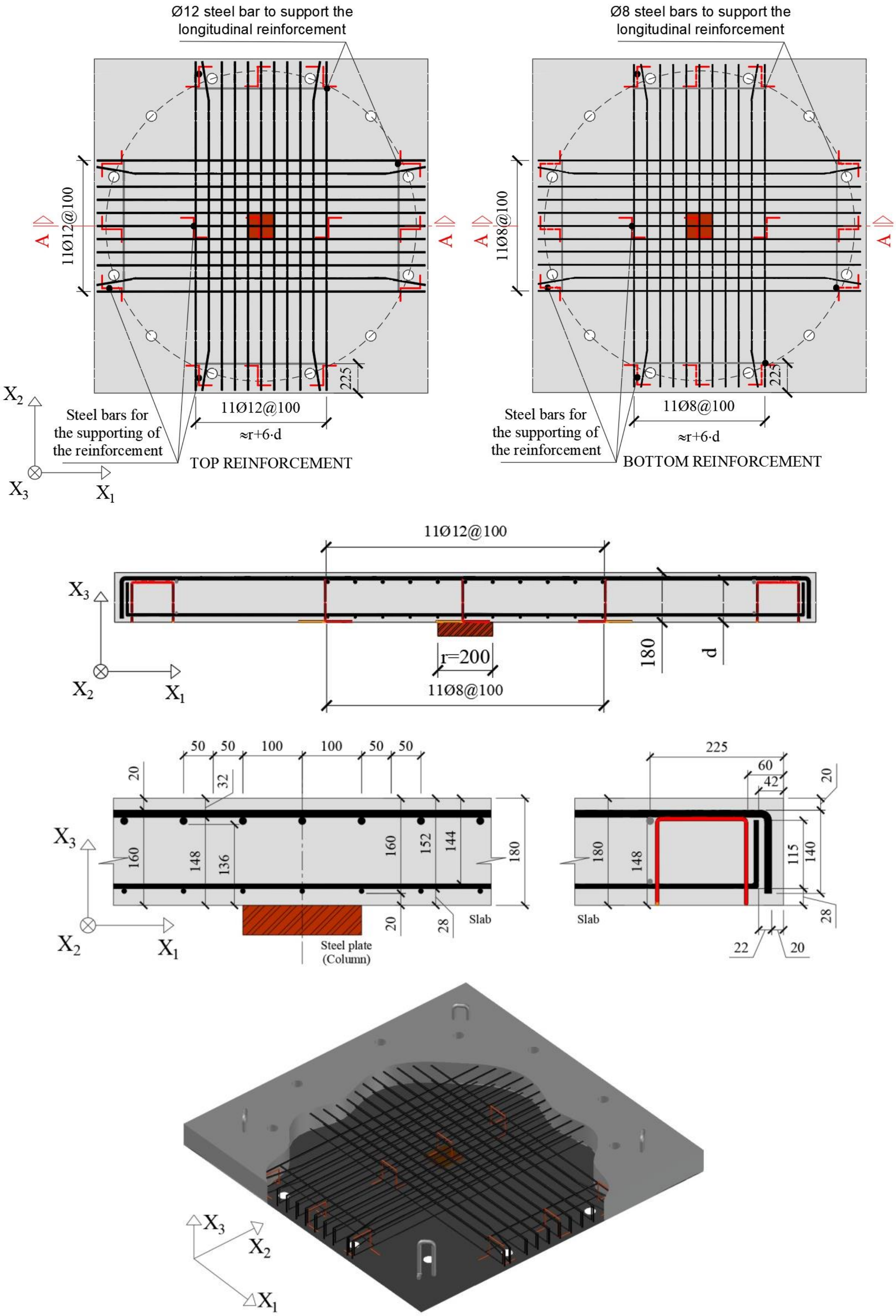

(c)

Figure 14 - (a) Geometry of the R/SFRC slab: cross-section (b) localization of the conventional reinforcement (c) details of the conventional reinforcement (dimensions in mm).

The test setup is shown in Figure 15, while the monitoring system is represented in Figure 16. During the tests, deflection will be measured in the points indicated in Figure 16a, and strains in the flexural reinforcements and in the SFRC will be recorded in electric strain gauges disposed as shown in Figure 16b and 16c, respectively. To monitor the applied load, a load cell will be installed in the extremity of the piston of the actuator. The maximum crack width will be determined through DIC technique in the region represented in Figure 16a. The results to be provided are the average of the two experimental tests.

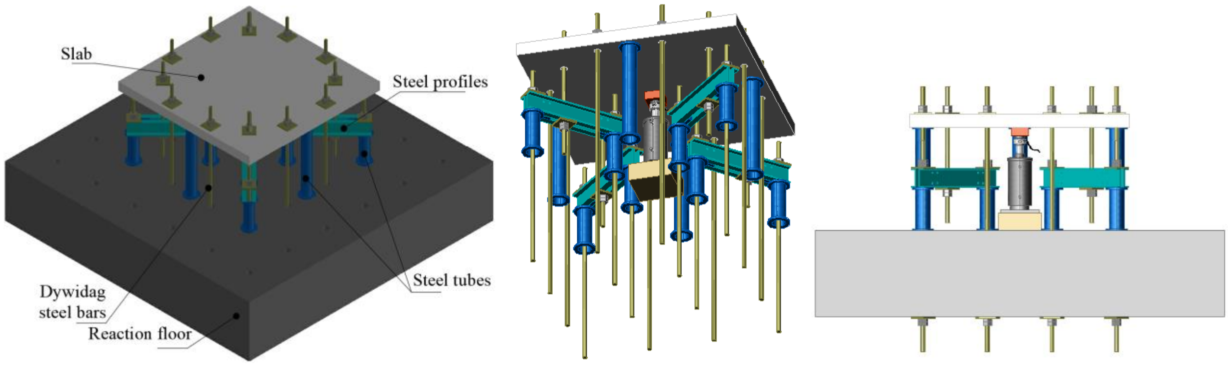

Figure 15 - Test setup of the R/SFRC slab prototypes.

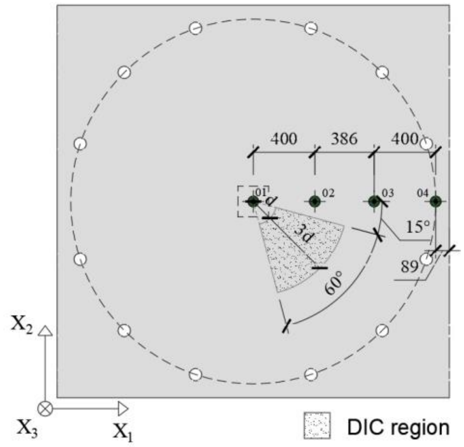

(a)

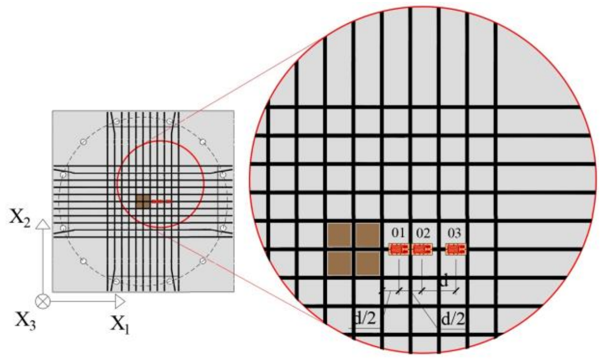

(b)

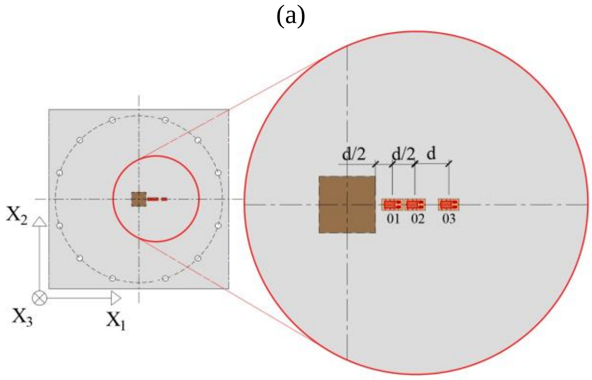

(c)

Figure 16 - Monitoring system: (a) points for measuring the deflections and zone for registering the average crack width; locations for measuring the strains in the (b) conventional reinforcements (top layer), and (c) in the R/SFRC slab's bottom surface (dimensions in mm).

The evaluation process will be like the one adopted in the previous BSC.

2.4.2 – 4th BSC: fibres for the transverse reinforcement of thin-walled tubular cross section elements subjected to torsion

In recent years, some developments on increasing the mechanical and durability properties of FRC have been done, with the purpose of using these composites in structural applications with the elimination of conventional steel reinforcements, mainly those more susceptible to corrosion, such is the case of steel stirrups, and, consequently, have lighter constructions systems [77]. To prevent corrosion, the use of fibre reinforcement polymer (FRP) reinforcements has been explored, in general in the form of GFRP bars [78, 79]. However, the smaller modulus of elasticity and bond conditions of these reinforcements erase some concerns on their use due to the extra difficulties they pose in terms of the verifications of the design prescriptions for SLS conditions, mainly deformability and crack opening [78-81]. The concern in terms of concrete crack opening is not related to the corrosion of the FRP reinforcements, but mainly on assuring the aggregate interlock resisting mechanism of concrete for the loadings of transverse nature, like shear, punching and torsion [82]. Due to the non-isotropic nature of the FRP, their dowel resisting mechanism when crossed by shear cracks is also smaller than the one guaranteed by steel reinforcements. Limiting the concrete crack width is also relevant, not only due to aesthetical concerns, but also the potential corrosion of steel fibres close to the surface of the elements, mainly above a certain crack width limit [83].

The application of FRP with a certain level of prestress can overcome part of the abovementioned concerns, by increasing the load at crack initiation, the stiffness of the elasto-cracked phase of the member, and its load carrying capacity at SLS conditions [78]. However, the tensile brittle nature of FRP and the susceptibility of their mechanical properties to high temperatures recommend the use of hybrid reinforcement, e.g., FRP plus steel, both applied with a certain level of prestress [78, 84, 85]. The steel reinforcement is disposed in the element with a cover thickness sufficient to minimize, as much as possible, its susceptibility to corrosion effects. Figure 17a shows a potential application of this material concept for thin-walled tubular cross section elements. This type of elements can be applied in the development of innovative constructions systems with technical and economic benefits, where their void part can be efficiently used for the installation of cables and/or pipes for functional requirements of the constructions that include these elements. These voids can also be reservoirs of rainwater to be used in case of a fire, by using proper sensors for triggering an effective irrigation system.

The 4th BSC will be dedicated to exploring, not only the structural performance of this material/structural concept, but also the performance of FEM-based models for predicting the behaviour at SLS and ULS conditions of an element that can be representative of this concept, when subject to a loading configuration that induces torsional effects, such is the one shown in Figure 17b (constant torsion and bending moment in the test zone).

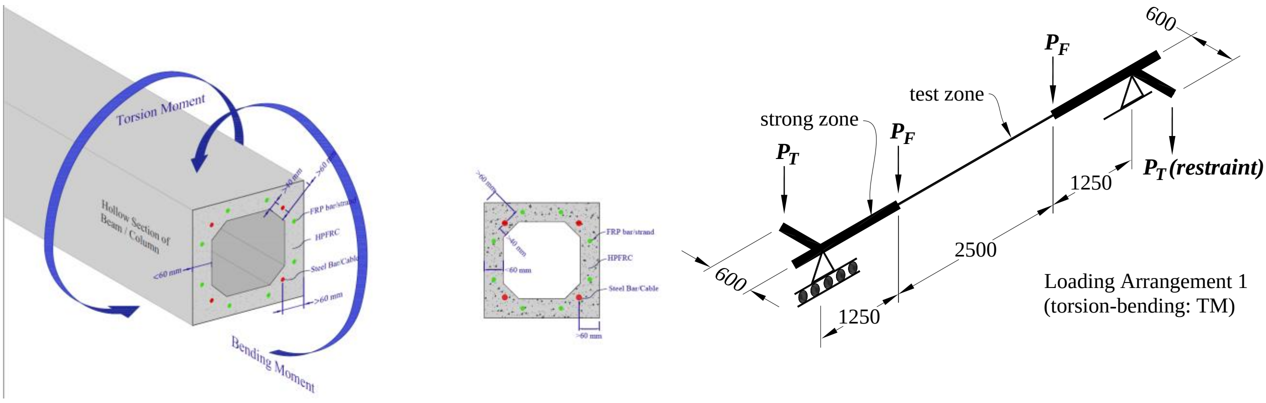

(a) (b)

Figure 17 – a) Thin-walled cross section tubular structural element in HPFRC with longitudinal hybrid reinforcement (FRP+steel); b) test setup for inducing a constant torsional and bending moment in the test region.

3 – FUTURE INITIATIVES OF THE *fib* WP 2.4.1

Each BSC is leading to a publication in an international journal for describing the relevant results and, based on the scores adopted to evaluate the predictive performance of the type of models adopted by the participants, important information has been extracted. However, the *fib* WP 2.4.1 has much larger ambition with the BSC activities. In fact, based on the scores in a BSC, the participations with the best scores per class of model (the representativeness is in proportion to the percentage of each class of model adopted in the competition) are invited to execute parametric studies with their models to evaluate the impact of the most relevant parameters of the models on the performance of the predictions. A report is prepared by each one of these selected teams of participants, according to proposed recommendations, and a final document resuming this sensitivity analysis is published. The *fib* WP2.4.1 believes that this exercise, extended to all BSC, will produce information of high value for the design practice of FRC structures with the types of FEM-based models used in the BSC.

Another activity *fib* WP2.4.1 is initiating in 2023 is related to the global resistance methods (GRM) for the design of FRC structures, whose application was recently explored to FRC structures [86]. Several GRM have been proposed for the design of RC structures with FEM-based models [87-91], namely: Partial Safety Factor (PSF), Global Resistance Factor (GRF), Method of estimating the coefficient of variation of the structural resistance (ECOV), and the Global Safety format (GSF). For this purpose, an elevate SFRC slab, experimentally tested and with suitable characterization of the

SFRC properties for design purpose, was already selected [92]. The members of the *fib* WP2.4.1, using different types of FEM-based models, will apply the GRM for the design of FRC structures to derive important conclusions about their potential. GRM will be also applied on the design of the structures tested in the BSC, as well as to R/FRC structures of large scale and of high potential use of FRC.

Another important objective of the *fib* WP2.4.1 is the formation of a COST initiative that helps to bring more members for the activities of this group, in order to help the development of a web-based application including a database with comprehensive, complete and reliable experimental tests of FRC structures, numerical simulations with FEM-based models and analysis of their predictive performance. The final aim is to have a web tool that can be used with machine learning (ML) algorithms for assisting in the determination of the most suited values of the FEM-based models on a reliable, safe, and economic design practice for taking advantage of fibre reinforcement for more sustainable built environment.

4 – CONCLUSIONS

The present paper describes the past, ongoing, and planned future initiatives of the *fib* WP 2.4.1 technical committee, which is dedicated to the design methodologies of fibre reinforced concrete (FRC) structures using software based on the finite element method. Focus was done on the blind simulation competitions (BSC) already executed, ongoing and planned for close future, and on the objectives behind these BSC. The final purpose of *fib* WP 2.4.1 is to derive knowledge for the development of innovative construction system by using FEM-based software that explores the potentialities of fibre reinforcement towards a more sustainable built environment.

ACKNOWLEDGEMENTS

The author acknowledges the support provided by FCT through the project FemWebAI, reference PTDC/ECI-EST/6300/2020, and by the Research Council of Lithuania (LMTLT) through the projects No. P-MIP-23-386 and No 01.2.2-LMT-K-718-03-0010 (from the European Regional Development Fund). This work was partly financed by FCT / MCTES through national funds (PIDDAC) under the R&D Unit Institute for Sustainability and Innovation in Structural Engineering (ISISE), under reference UIDB/04029/2020, and under the Associate Laboratory Advanced Production and Intelligent Systems ARISE under reference LA/P/0112/2020.

REFERENCES

[1] *fib* Bulletin 105, "Fibre reinforced concrete", State-of-the-Art-report prepared by Task Group 4.1 "Fibre-reinforced concrete" and Task Group 4.2 "Ultra-high-performance fibre-reinforced concrete", 2022.

[2] ACI 544.6R-15, "Report on design and construction of steel fiber-reinforced concrete elevated slabs", Reported by ACI Committee 544, 2015.

[3] - Taheri, M.; Barros, J.A.O.; Salehian, H., "Integrated approach for the prediction of crack width and spacing in flexural FRC members with hybrid reinforcement", Engineering Structures, 110208, 2020. https://doi.org/10.1016/j.engstruct.2020.110208

[4] ACI SP-319 Technical Publication, Symposium Volume on the Reduction of Crack Width with Fiber, Editors: Corina-Maria Aldea and Mahmut Ekenel, ACI, ISBN-13: 978-1-945487-68-2, SP-319-2 chapter, 2017.

[5] Abrishambaf, A.; Barros, J.A.O.; and Cunha, V.M.C.F., "Time-dependent flexural behavior of cracked steel fibre reinforced self-compacting concrete panels", *Cement and Concrete Research*, Vol. 72, 21–36, 2015.

[6] Tiberti, G.; Minelli, F.; Plizzari, G.A., "Cracking behavior in reinforced concrete members with steel fibers: A comprehensive experimental study", *Cement and Concrete Research*, Vol. 68, ISSN: 0008-8846, pp. 24-34, 2015.

[7] Vasanelli, E.; Micelli, F.; Aiello, M. A.; Plizzari, G., "Crack width prediction of FRC beams in short and long term bending condition", *Materials and Structures*, Vol. 47, No. 1-2, pp 39-54, 2014.

[8] Vandewalle, L., "Cracking behaviour of concrete beams reinforced with a combination of ordinary reinforcement and steel fibres", *Materials and Structures*, Vol. 33, April 2000, pp. 164-170, 2000.

[9] Sousa, C.; Barros, J.A.O.; Correia, J.P.R.R.; "In-plane cyclic behaviour of RC frames strengthened with composite sandwich panels", Engineering Structures Journal, 251, 113529, 2022. https://doi.org/10.1016/j.engstruct.2021.113529

[10] Lameiras, R.M.; Barros, J.A.O.; Valente, M.I.B.; Poletti, E.; Azevedo, M.; Azenha, M.A.D., "Seismic behaviour of precast sandwich wall panels of steel fibre reinforced concrete layers and fibre reinforced polymer connectors", Engineering Structures Journal, 237, 112149, 2021. https://doi.org/10.1016/j.engstruct.2021.112149

[11] Caballero-Morison, K.E.; Bonet, J.L.; Navarro-Gregori, J.; Martí-Vargas, J.R., "Behaviour of steel fibre-reinforced normal-strength concrete slender columns under cyclic loading", *Engineering Structures*, Vol. 39, pp. 162-175, 2012.

[12] Li, Y.; Aoude, H., "Influence of steel fibers on the static and blast response of beams built with high-strength concrete and high-strength reinforcement", Engineering Structures, 221, 111031, 2020.

[13] Cadoni, E.; Forni, D.; Bonnet, E.; Dobrusky, S., "Experimental study on direct tensile behaviour of UHPFRC under high strain-rates", Construction and Building Materials, 218, 667-80, 2019.

[14] Hao, Y.; Hao, H., "Mechanical properties and behaviour of concrete reinforced with spiral-shaped steel fibres under dynamic splitting tension", Magazine of Concrete Research, 68, 1110-21, 2016.

[15] Yoo, D.Y.; Banthia, N.; Kang, S.T.; Yoon, Y.S., "Effect of fiber orientation on the rate-dependent flexural behavior of ultra-high-performance fiber-reinforced concrete", Composite Structures, 157, 62-70, 2016.

[16] Dancygier, A.N.; Katz, A.; Benamou, D.; Yankelevsky, D.Z., "Resistance of double-layer reinforced HPC barriers to projectile impact", International Journal of Impact Engineering, 67, 39-51, 2014.

[17] Zhang, X.X.; Abd Elazim A.M.; Ruiz, G.; Yu, R.C., "Fracture behaviour of steel fibre-reinforced concrete at a wide range of loading rates", International Journal of Impact Engineering, 71,89-96, . 2014.

[18] Almusallam, T.H.; Siddiqui, N.A.; Iqbal, R.A.; Abbas, H., "Response of hybrid-fiber reinforced concrete slabs to hard projectile impact", International Journal of Impact Engineering, 58, 17-30, . 2013.

[19] Caverzan, A.; Cadoni, E.; di Prisco, M., "Tensile behaviour of high performance fibre-reinforced cementitious composites at high strain rates", International Journal of Impact Engineering, 45, 28-38, . 2012.

[20] Colombo, M.; di Prisco, M.; Felicetti, R., "SFRC exposed to high temperature: Hot vs. residual characterization for thin walled elements", Cement and Concrete Composites, 58, 81-94, 2015.

[21] Balázs, G.L.; Lublóy, É., "Post heating strength of fibre-reinforced concretes", Fire Safety Journal, 49, DOI: 10.1016/j.firesaf.2012.01.002, 2012.

[22] ACI 544.5R-10, "Report on the Physical Properties and Durability of Fiber-Reinforced Concrete", American Concrete Institute, Farmington Hills, 2010.

[23] Alsaif, A.; Bernal, S.A.; Guadagnini, M.; Pilakoutas, K., "Durability of steel fibre reinforced rubberised concrete exposed to chlorides", Construction and Building Materials, 188, 130-142, 2018.

[24] Sofi, A., "Effect of waste tyre rubber on mechanical and durability properties of concrete – A review", Ain Shams Engineering Journal, 9, 2691-2700, 2018.

[25] Marcos-Meson, V.; Michel, A.; Solgaard, A.; Fischer, G.; Edvardsen, C.; Skovhus, T.L., "Corrosion resistance of steel fibre reinforced concrete – A literature review", Cement and Concrete Research, 103, 1-20, 2018.

[26] Thomas, B.S.; Gupta, R.C.; Panicker, V.J., "Recycling of waste tire rubber as aggregate in concrete: durability-related performance", Journal of Cleaner Production, 112, 504-513, 2016.

[27] Masmoudi, A.; Bouaziz, J., "Durability of Steel Fibres Reinforcement Concrete Beams in Chloride Environment Combined with Inhibitor", Hindawi Publishing Corporation, Advances in Materials Science and Engineering, Article ID 1743952, 6 pages, 2016.

[28] Frazão, C.; Camões, A.; Barros, J.; Gonçalves, D., "Durability of steel fiber reinforced self-compacting concrete", Construction and Building Materials, 80, 155-166, 2015. https://doi.org/10.1016/j.conbuildmat.2015.01.061

[29] Shi, X.; Xie, N.; Fortune, K.; Gong, J., "Durability of steel reinforced concrete in chloride environments: An overview", Construction and Building Materials, 30, 125-138, 2012.

[30] Nordström, E., "Durability of Sprayed Concrete – Steel fibre corrosion in cracks", Doctoral Thesis, Department of Civil and Environmental Engineering, Division of Structural Engineering, Luleå University of Technology, Sweden, 2005.

[31] Frazão, C.M.V.; Barros, J.A.O.; Bogas, J.A.B.A., "Technical and environmental potentialities of recycled steel fibers for structural applications", Journal of Building Engineering, 45, 103579, 2022. https://doi.org/10.1016/j.jobe.2021.103579

[32] Pawelska-Mazur, M.; Kaszynska, M., "Mechanical Performance and Environmental Assessment of Sustainable Concrete Reinforced with Recycled End-of-Life Tyre Fibres", Materials, 14, 256, 2021. https://doi.org/10.3390/ma14020256

[33] Pushkar, S.; Ribakov, Y., "Life-Cycle Assessment of Strengthening Pre-Stressed Normal-Strength Concrete Beams with Different Steel-Fibered Concrete Layers", Sustainability 2020, 12(19), 7958, 2020. https://doi.org/10.3390/su12197958

[34] Maxineasa, S.G.; Neocleous, K.; Dumitrescu, L.; Themistocleous, K.; Taranu, N.; Hadjimitsis, D., "Environmental LCA of innovative reuse of all end-of-life tyre components in concrete", Proceeding of the 1st International Conference on Construction Materials for Sustainable Future, Zadar, Croatia, 19-21 April 2017, ISBN: 978-953-8168-04-8, pp 941-947.

[35] Bentur, A.; Mindess, S., "Fibre Reinforced Cementitious Composites", 2nd edition, Francis & Taylor, UK, 2007.

[36] Chen Y.; Cen G.; Cui, Y. , "Comparative analysis on the anti-wheel impact performance of steel fiber and reticular polypropylene synthetic fiber reinforced airport pavement concrete under elevated temperature aging environment", Construction and Building Materials 192, 818–835, 2018, ISSN 09500618, doi: 10.1016/j.conbuildmat.2018.10.175.

[37] Yang, M.; Shin, H.-O.; Yoo, D.-Y., "Benefits of using amorphous metallic fibers in concrete pavement for long-term performance", Archives of Civil and Mechanical Engineering 17 (4), 750–760, 2017, ISSN 16449665, doi: 10.1016/j.acme.2017.02.010.

[38] Nobili, A.; Lanzoni, L.; Tarantino, A.M., "Experimental investigation and monitoring of a polypropylene-based fiber reinforced concrete road pavement", Construction and Building Materials, 47, 888-895, 2013.

[39] Conforti, A.; Tiberti G.; Plizzari, G.A.; Caratelli, A.; Meda, A., "Precast tunnel segments reinforced by macro-synthetic fibers", Tunnelling and Underground Space Technology journal, 63, 1-11, 2017.

[40] Craig, R., "Malmo's constructions starts", Tunneling & Trenchless Construction, 12-14, 2006.

[41] Craig, R., "Dartford cable tunnel", Tunneling & Trenchless Construction, 17-19, 2004.

[42] Soetens, T., "Design models for the shear strength of prestressed precast steel fibre reinforced concrete girders", PhD thesis, Gent University, 2015.

[43] de la Fuente, A.; Escariz, R.; de Figueiredo, A.; Aguado, A., "Design of macro-synthetic fiber reinforced concrete pipes", Construction and Building Materials 43, 523–532, 2013.

[44] Laranjeira, F., "Design-oriented constitutive model for steel fiber reinforced concrete", PhD Thesis, Universitat Politècnica de Catalunya, Spain, 2010.

[45] Carvalho, M.R.; Barros, J.A.O.; Zhang, Y.; Dias-da-Costa, D., "A computational model for simulation of steel fibre reinforced concrete with explicit fibres and cracks", Computer Methods in Applied Mechanics and Engineering, Elsevier, 363: 112879, 2020 (doi: https://doi.org/10.1016/j.cma.2020.112879).

[46] Chi, Y.; Yu, M.; Huang, L.; Xu, L., "Finite element modeling of steel-polypropylene hybrid fiber reinforced concrete using modified concrete damaged plasticity", Engineering Structures, 148, 23-35, 2017.

[47] Zhan, Y.; Meschke, G.; "Adaptive Crack Modeling with Interface Solid Elements for Plain and Fiber Reinforced Concrete Structures". Materials, 10(7), 771, 2017.

[48] Teixeira, M.D.E.; Barros, J.A.O.; Cunha, V.M.C.F.; Moraes-Neto, B.N.; Ventura-Gouveia, A., "Numerical simulation of the punching shear behaviour of self-compacting fibre reinforced flat slabs", Construction and Building Materials journal, 74, 25-36, January 2015. DOI: 10.1016/j.conbuildmat.2014.10.003. http://hdl.handle.net/1822/38262

[49] Deluce, J. R.; Lee, S. C.; Vecchio, F. J., "Crack Model for Steel Fiber-Reinforced Concrete Members Containing Conventional Reinforcement", ACI Structural Journal, 111(1), 93–102, 2014. https://doi.org/10.14359/51686433

[50] Cunha, V.M.C.F.; Barros, J.A.O.; Sena-Cruz, J.M., "A finite element model with discrete embedded elements for fibre reinforced composites", Computers and Structures Journal, 94-95, 22-33, 2012.

[51] Oliver, J.; Mora, D.F.; Huespe, A.E.; Weyler, R., "A micromorphic model for steel fiber reinforced concrete", International Journal of Solids and Structures, 49(21): 2990-3007, 2012.

[52] Padmarajaiah, S.K.; Ramaswamy, A., "A finite element assessment of flexural strength of prestressed concrete beams with fibre reinforcement", Cement and Concrete Composites, 24, 229-241, 2002.

[53] Gudzulic, V.; Dang, T.; Meschke, G., "Computational modeling of fiber flow during casting of fresh concrete", Computational Mechanics, 63(6), 1111-1129, 2018.

[54] E. Denneman, R. Wu, E. P. Kearsley, A. T. Visser, Discrete fracture in high performance fibre reinforced concrete materials, Engineering Fracture Mechanics 78 (10) (2011) 2235–2245, ISSN 00137944, doi: 10.1016/j.engfracmech.2011.04.008.
[55] Matos, L.M.P.; Barros, J.A.O.; Ventura-Gouveia, A.; Calçada, R., "A new inverse analysis approach for predicting the fracture mode I parameters of fibre reinforced concrete", Engineering Fracture Mechanics Journal, Volume 246, 1 April 2021, 107613, https://doi.org/10.1016/j.engfracmech.2021.107613.
[56] Salehian, H.; Barros, J.A.O., "Assessment of the performance of steel fibre reinforced self-compacting concrete in elevated slabs", Cement and Concrete Composites, 55, 268-280, January 2015. DOI: 10.1016/j.cemconcomp.2014.09.016. http://hdl.handle.net/1822/38275
[57] Jang, S.-J.; Jeong, G.-Y.; Yun, H.-D., "Use of steel fibers as transverse reinforcement in diagonally reinforced coupling beams with normal- and high-strength concrete", Construction and Building Materials 187, 1020–1030, 2018, ISSN 09500618, doi: 10.1016/j.conbuildmat.2018.08.063.
[58] Barros, J.A.O.; Foster, S., "An integrated approach for predicting the shear capacity of fibre reinforced concrete beams", Engineering Structures Journal, 174, 346-357, 2018. https://doi.org/10.1016/j.engstruct.2018.07.071.
[59] Amin, A.; Foster, S.J. "Shear strength of steel fibre reinforced concrete beams with stirrups", Engineering Structures, 111:323–32, 2016
[60] Singh, B.; Jain, K. "Appraisal of steel fibers as minimum shear reinforcement in concrete beams", ACI Structural Journal, 111(5):1191–202, 2014
[61] Minelli, F., Conforti, A., Cuenca, E., Plizzari, G.A. (2014), "Are steel fibres able to mitigate or eliminate size effect in shear?", Materials and Structures, Vol. 47, No. 3, pp. 459-473.
[62] Conforti, A.; Minelli, F.; Plizzari, G.A. "Wide-shallow beams with and without steel fibres: a peculiar behaviour in shear and flexure", Composites Part B Engineering, 51:282–90, 2013
[63] Minelli, F., & Plizzari, G.A. (2013), "On the effectiveness of steel fibres as shear reinforcement", ACI Structural Journal, Vol. 110, No 3, May-June 2013, pp. 379-389, ISSN 0889-3241.
[64] Aoude, H.; Belghiti, M.; Cook, W.D.; Mitchell, D. "Response of steel fiber-reinforced concrete beams with and without stirrups", ACI Structural Journal,109(3):359–68, 2012
[65] Lee, H.H. (2007), "Shear strength and behavior of steel fiber reinforced concrete columns under seismic loading", Engineering Structures, Vol. 20, pp. 1253–1262.
[66] Kwak, Y-K; Eberhard, MO; Kim W-S; Kim J. "Shear strength of steel fiber-reinforced concrete beams without stirrups", ACI Structural Journal, 99(4):530–8, 2002
[67] Barros, J.A.O.; Moraes-Neto, B.N.; Melo, G.S.S.A.; Frazão, C.M.V., "Assessment of the effectiveness of steel fibre reinforcement for the punching resistance of flat slabs by experimental research and design approach", Composites Part B Journal, 78, 8-25, September 2015. http://dx.doi.org/10.1016/j.compositesb.2015.03.050
[68] Maya Duque, L. F., Fernández Ruiz, M., Muttoni A., Foster, S. J. (2012), "Punching shear strength of steel fibre reinforced concrete slabs", *Engineering Structures*, Vol. 40, UK, pp. 93-94.
[69] *fib* Bulletin 57 (2010), "Shear and punching shear in RC and FRC elements", *Proc. Workshop held in Salò*, Brescia, Italy.
[70] Choi, K-K., Taha, M.M.R., Park, H-G., Maji, A.K. (2007), "Punching shear strength of interior concrete slab-column connections reinforced with steel fibers", *Cement & Concrete Composites*, Vol. 29, No. 5, pp. 409-420.

[71] NP EN 12390-3:2011. Testing hardened concrete - Part 3: Compressive strength of test specimens.
[72] NP EN 12390-13:2014. Testing hardened concrete - Part 13: Determination of secant modulus of elasticity in compression.
[73] *fib* Model Code 2010: *fib* Model Code for Concrete Structures 2010.
[74] NP EN ISO 6892-1:2016. Metallic materials - Tensile testing - Part 1: Method of test at room temperature.
[75] Barros, J.A.O., Sanz, B.; Kabele, P.; Yu, R.C.; Meschke, G.; Planas, J.; Cunha, V.; Caggiano, A.; Ozyurt, N.; Ventura-Gouveia, A.; Bos, A.V.D.; Poveda, E.; Gal, E.; Cervenka, J.; Ney, G.E.; Rossi, P.; Dias-da-Costa, D.; Juhasz, P.K.; Cendon, D.; Ruiz, G.; Valente, T., "Blind competition on the numerical simulation of steel fibre reinforced concrete beams failing in shear", fib Structural Concrete Journal, 22(2), 939-967, 2021. http://dx.doi.org/10.1002/suco.202000345
[76] Barros, J.A.O., Sanz, B.; Filho, M.M.; Figueiredo, F.P.; Kabele, P.; Yu, R.C.; Meschke, G.; Planas, J.; Cunha, V.; Caggiano, A.; Ozyurt, N.; Ventura-Gouveia, A.; Bos, A.V.D.; Poveda, E.; Gal, E.; Cervenka, J.; Neu, G.E.; Rossi, P.; Dias-da-Costa, D.; Juhasz, P.K.; Cendon, D.; Ruiz, G.; Valente, T., "Blind competition on the numerical simulation of continuous shallow steel-fibre reinforced concrete beams failing in bending", *fib* Structural Concrete Journal, 2023. https://doi.org/10.1002/suco.202200754
[77] Barros, J.A.O., "Fiber reinforced concrete and glass fibre reinforced polymer systems for the development of more sustainable construction systems", BEFIB 2016, 9th Rilem International Symposium on Fiber Reinforced Concrete, Vancouver, Canada, 19-21 September 2016 (Invited paper for the Special Session in honour of Prof. Horst Falkner).
[78] Mazaheripour, H.; Barros, J.A.O.; Soltanzadeh, F.; Sena-Cruz, J.M., "Deflection and cracking behavior of SFRSCC beams reinforced with hybrid prestressed GFRP and steel reinforcements", Engineering Structures journal, 125, 546-565, October 2016. http://dx.doi.org/10.1016/j.engstruct.2016.07.026.
[79] Barris, C.; Torres, L.; Turon, A.; Baena, M.; and Catalan, A., "An experimental study of the flexural behaviour of GFRP RC beams and comparison with prediction models", Composite Structures, 91(3), 286-295, 2009.
[80] Harajli, M. and Abouniaj, M., "Bond performance of GFRP bars in tension: Experimental evaluation and assessment of ACI 440 guidelines", Journal of Composites for Construction 14(6), 659-668, 2010.
[81] Mazaheripour, H.; Barros, J.A.O.; Sena-Cruz, J.M.; Pepe, M.; Martinelli, E., "Experimental study on bond performance of GFRP bars in self-compacting steel fiber reinforced concrete", Composite Structures Journal, 95, 202-212, 2013.
[82] Kaszubska, M.; Kotynia, R.; Barros, J.A.O.; Baghi, H., "Shear behavior of concrete beams reinforced exclusively with longitudinal GFRP bars: experimental research", Structural Concrete, fib journal, February 2018. DOI: 10.1002/suco.201700174.
[83] Technical Note, "Effects of steel fiber corrosion on durability and long-term mechanical performance of FRC", prepared by the ACI 544.E technical committee of ACI, 2022
[84] Qu, W.; Zhang, X.; and Huang, H., "Flexural Behavior of Concrete Beams Reinforced with Hybrid (GFRP and Steel) Bars*",* Journal of Composites for Construction 13(5), 350-359, 2009.
[85] Leung, H.; Balendran, R., "Flexural behaviour of concrete beams internally reinforced with GFRP rods and steel rebars", Structural Survey, 21(4), 146-157, 2003.
[86] Neu, G.E.; Gudzulic, V.; Meschke, G., "Design of steel fiber reinforced concrete tunnel lining segments by nonlinear finite-element analysis with different safety formats", Computational Modelling of Concrete and Concrete Structures, Meschke, Pichler, & Rots (Eds), DOI 10.1201/9781003316404-88.

[87] *fib* Model Code for Concrete Structures 2010 [Internet]. John Wiley & Sons; 402 p.2013 [cited 2018 Jun 4]. Available from: https://onlinelibrary.wiley.com/doi/book/10.1002/9783433604090
[88] Cervenka, V., "Global safety formats in fib Model Code 2010 for design of concrete structures", [Internet], 2013 [cited 2021 Mar 6]. Available from: /paper/Global-safety-formats-in-fib-Model-Code-2010-for-of-Cervenka/9391b218e95988232c7a4d1e36268784aab9693e
[89] Allaix, D.L.; Carbone, V.I.; Mancini, G., "Global safety format for non-linear analysis of reinforced concrete structures", Structural Concrete, 14(1), 29–42, 2013.
[90] Pimentel, M.; Brühwiler, E.; Figueiras, J., "Safety examination of existing concrete structures using the global resistance safety factor concept", Engineering Structures, 70:130–43, 2014.
[91] Castaldo, P.; Gino, D.; Mancini, G., "Safety formats for non-linear finite element analysis of reinforced concrete structures: discussion, comparison and proposals", Engineering Structures, 193:136–53, 2019.
[92] Aidarov, A.; Mena, F.; de la Fuente, A., "Structural response of a fibre reinforced concrete pile-supported flab slab: full-scale test, "Engineering Structures, 239, 112292, July 2021, https://doi.org/10.1016/j.engstruct.2021.112292.